ACS SyntheticBiology

Research Article

pubs.acs.org/synthbio

Gene Expression Platform for Synthetic Biology in the Human Pathogen *Streptococcus pneumoniae*

Robin A. Sorg, Oscar P. Kuipers, and Jan-Willem Veening*

Molecular Genetics Group, Groningen Biomolecular Sciences and Biotechnology Institute, Centre for Synthetic Biology, University of Groningen, Nijenborgh 7, 9747 AG, Groningen, The Netherlands

ABSTRACT: The human pathogen *Streptococcus pneumoniae* (pneumococcus) is a bacterium that owes its success to complex gene expression regulation patterns on both the cellular and the population level. Expression of virulence factors enables a mostly hazard-free presence of the commensal, in balance with the host and niche competitors. Under specific circumstances, changes in this expression can result in a more aggressive behavior and the reversion to the invasive form as pathogen. These triggering conditions are very difficult to study due to the fact that environmental cues are often unknown or barely possible to simulate outside the host (*in vitro*). An alternative way of investigating expression patterns is found in synthetic biology approaches of reconstructing regulatory networks that mimic an observed behavior with orthogonal components. Here, we created a genetic platform suitable for synthetic biology approaches in *S. pneumoniae* and characterized a set of standardized promoters and reporters. We show that our system allows for fast and easy cloning with the BglBrick system and that reliable and robust gene expression after integration into the *S. pneumoniae* genome is achieved. In addition, the cloning system was extended to allow for direct linker-based assembly of ribosome binding sites, peptide tags, and fusion proteins, and we called this new generally applicable standard "BglFusion". The gene expression platform and the methods described in this study pave the way for employing synthetic biology approaches in *S. pneumoniae*.

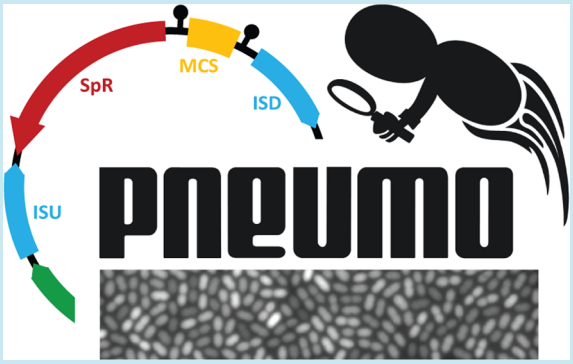

KEYWORDS: *BioBrick, BglFusion, Golden Gate Shuffling, luciferase, GFP, mKate2*

The Gram-positive bacterium *Streptococcus pneumoniae* (pneumococcus) is a colonizer of the human nasopharynx that can be found in up to 50% of children[1] and 10% of adults.[2] In the case of an intact and alert immune system, *S. pneumoniae* represents no direct threat and is thus considered a commensal.[3] Nevertheless, pneumococci needed to develop strategies to hide or resist the immune system to be able to survive within the human body. These adaptations can lead to pathogenic behavior when encountering immune systems that are inexperienced or weak, as in the case of young children or old and immunocompromised adults. The diseases caused by *S. pneumoniae* span from otitis media and sinusitis to the life-threatening meningitis, sepsis, and pneumonia that cause more than one million deaths per year.[4]

In the era of systems biology, one big question in pneumococcal research focuses on virulence factors and their regulation of activity. Virulence factors comprise all genes that manipulate the host, particularly, immune system functions. Gene expression regulatory networks that evolved in such interactive environments are very difficult to study *in vitro* due to the fact that culture media are optimized for robust growth and lack the complexity and signaling cues that cells experience *in vivo*. One alternative way of studying complex patterns can be found in synthetic biology approaches, where regulatory networks of interest are replaced by synthetic circuits of well-characterized orthogonal components.[5] This strategy allows for the use of chemicals as inducer molecules driving for example noisy switches that activate virulence factors such as an increased capsule production. Regulation patterns that lead to the establishment of two metabolically distinguishable populations (in the mentioned example of increased capsule production referred to as phase variation) are suspected to be critical in impeding the success of one single specific immune response.[6] A comparative analysis of native and synthetic circuits can also give information about the importance of network architecture in contrast to parametrization of individual components. For instance, Çağatay et al. built a synthetic gene regulatory pathway that drives competence development in *Bacillus subtilis* that was more precise than the natural network.[7] Interestingly, cells having the natural, noisy network had higher transformation efficiencies under variable conditions demonstrating why noise in competence development might have evolved.[7] The global idea of using synthetic biology to gain insights into biological processes such as bacterial pathogenesis is nicely described by the famous quote of Richard Feynman: What I cannot create I do not understand. The study of the colonization success of a pneumococcal population with differential capsule expression under control of

Received: November 14, 2013
Published: May 20, 2014

a synthetic regulatory network would, for example, represent such an approach. Comparisons to the wild type might shed light on the mechanism and moreover on the relevance of the native control system, whose mode of operation is still unknown.

An introduction of engineering principles to molecular biology promises to represent a critical step both toward a deeper understanding of cellular mechanisms as well as toward real applications by programming synthetic circuits with designed characteristics.[8] The pneumococcus is an organism with good prospects in this field, since it has a relatively small genome of approximately 2 Mb, it becomes naturally competent for transformation, and there are well-established assays for both *in vitro* and animal studies. The first step to launch *S. pneumoniae* as a chassis for synthetic biology studies relies in the creation of a standard gene expression platform in the form of an integration plasmid that allows for rapid and robust assembly of genetic components. In a second step, individual components need to be characterized to enable free shuffling of predictable biological functions.

A major bottleneck of studying microorganisms remains efficient DNA assembly. The most common task in this process is the combination of two sequences in a single reaction, while leaving the possibility of adding more constructs in an iteration of the very same process. BglBrick cloning,[9] a variant of the more commonly known BioBrick cloning,[10] solves this problem by using restriction enzymes with compatible ends flanking individual genetic elements - *Bgl*II at the 5′ and *Bam*HI at the 3′ end. When combining two elements, a scar sequence is created that is no longer recognized by these two enzymes while the pattern of the composite part with 5′ *Bgl*II and 3′ *Bam*HI becomes re-established. The BglBrick scar codes for a glycine and a serine residue while the original BioBrick standard scar results in a tyrosine followed by a stop codon. For this reason, we chose BglBrick cloning as our preferred standard. Multiple genetic elements, as in case of entire vectors, can also be assembled in a single reaction with strategies such as Golden Gate Shuffling.[11] With this study, we aim to introduce these techniques into the *Streptococcus pneumoniae* field.

The plasmid pPEP1 (Pneumococcal Engineering Platform) was created that allows for chromosomal integration in the pathogenic serotype 2 encapsulated *S. pneumoniae* strain D39[12] and its commonly used nonpathogenic unencapsulated derivatives such as strains R6, R800, and Rx1. Vector components that lack restriction sites for BglBrick cloning were PCR amplified from genome, plasmids, and synthetic sequences and assembled via Golden Gate Shuffling. Subcloning was carried out in *Escherichia coli* strain MC1061. Constitutive synthetic promoters of different strengths, and the fucose, maltose, and Zn^{2+}-inducible promoters, were characterized using bioluminescence assays employing firefly luciferase and fluorescence reporters. In addition, a new trehalose-inducible promoter is reported. Finally, we improved the BglBrick standard and introduced specific sequences that allow for direct linker-based assembly of ribosome binding sites, peptide tags, and fusion proteins; we call this new standard BglFusion. We show that this novel genetic platform offers robust and easy cloning and confers reliable expression within the pneumococcal genome paving the way for synthetic biology approaches in this important human pathogen.

RESULTS AND DISCUSSION

Vector Construction and Assembly. We designed and build up a vector by combining PCR amplified genomic parts, plasmid parts, and synthetic sequences. The main idea behind the choice for individual vector components relied in creating a chromosomal integration platform in *S. pneumoniae* while at the same time allowing for plasmid propagation in both Gram-positive and Gram-negative backgrounds. To meet the requirements of combinatorial cloning, the presence of recognition sites for BglBrick restriction enzymes (*Eco*RI, *Bgl*II, *Bam*HI and *Xho*I) were eliminated in the individual parts. The modular vector consists of 7 individual components (Figure 1A): two embracing homology regions for double

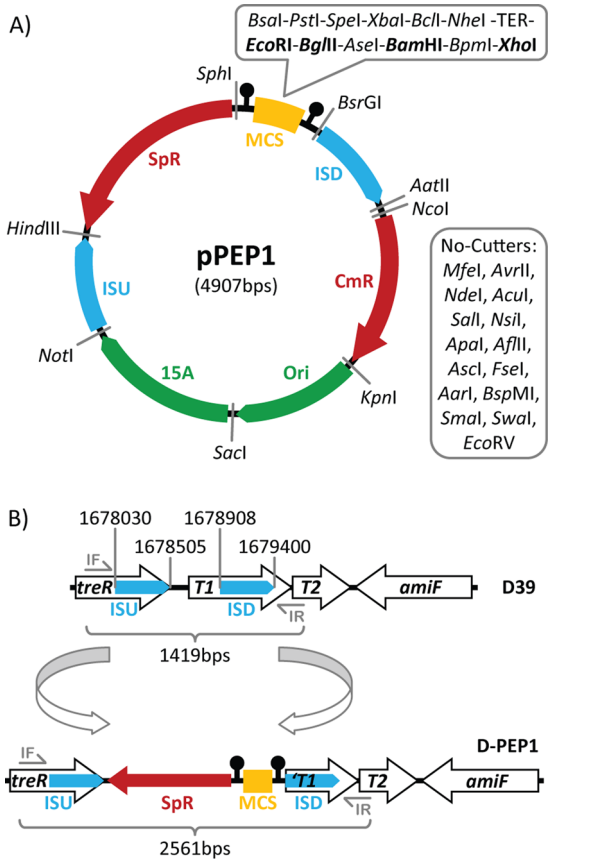

Figure 1. Plasmid and integration map of pPEP1. (A) Construction map of pPEP1 including all relevant single cutting and a selection of noncutting restriction sites. The BglBrick enzymes are depicted in bold. Terminators (black circles) in both reading directions insulate the MCS. Furthermore, the MCS is intersected by terminators (TER) to allow the simultaneous activity of two expression units with minimal reciprocal interference. (B) pPEP1 integration through double crossover into the *S. pneumoniae* D39 chromosome. The base pair positions of the two homology sequences are indicated and correct double crossover recombination can be verified with the primer pair IF/IR, which both bind the genome outside the homology sequences present on pPEP1.

crossover integration in the pneumococcal chromosome located at opposite sides of the plasmid named integration site up (ISU) and integration site down (ISD); the multiple cloning site (MCS) and an antibiotic resistance cassette (in this case conferring spectinomycin resistance; SpR) present within the integration sequences; two different origins of replication for plasmid propagation (15A and Ori) and an additional

dx.doi.org/10.1021/sb500229s | ACS Synth. Biol. 2015, 4, 228−239

Table 1. Primers/Oligonucleotides[a]

name	sequence		restriction sites
A-F/R:	5'-gcatcGGTCTC^{1}a**gttg**TGTACA^3*(n)*$_{ISD}$ -3'	5'-gcatcGGTCTC^{1}a**caac**GCATGC^2*(n)*$_{SpR}$ -3'	
B-F/R:	5'-gcatcGGTCTC^{1}a**ctga**CCATGG^5*(n)*$_{CmR}$ -3'	5'-gcatcGGTCTC^{1}a**tcag**GACGTC^4*(n)*$_{ISD}$ -3'	
C-F/R:	5'-gcatcGGTCTC^{1}a**accg**GAGCTC^7*(n)*$_{15A}$ -3'	5'-gcatcGGTCTC^{1}a**cggt**GGTACC^6*(n)*$_{CmR}$ -3'	
D-F/R:	5'-gcatcGGTCTC^{1}a**gcta**gGCGGCCGC^8*(n)*$_{ISU}$ -3'	5'-gcatcGGTCTC^{1}a**tagc***(n)*$_{15A}$ -3'	
E-F/R:	5'-gcatcGGTCTC^{1}a**tggc**tagaAAGCTT^9*(n)*$_{SpR}$-3'	5'-gcatcGGTCTC^{1}a**gcca***t(n)*$_{ISU}$ -3'	
MCS-F/R:	5'-gcattG**CATGC**^{2}*(n)*$_{MCS}$ -3	5'-gcatgT**GTACA**^{3}*(n)*$_{MCS}$ -3'	
Ori-F/R:	5'-gcattG**GTACC**^{6}*(n)*$_{Ori}$ -3'	5'-cgtcaG**AGCTC**^{7}*(n)*$_{Ori}$ -3'	
IF/IR:	5'-*ccaacctaaccagctaccaag*-3'	5'-*catggcacggctaagatgttg*-3'	
CDS-F/R:	5'-gctggAT**TA***ATg(n)*$_{CDS}$ -3'	5'-gcatgG**GATC***Cttattatta(n)*$_{CDS}$ -3'	*Ase*I/*Bam*HI
RBS-F/R:	5'-**AATT***CatgAGATCT(n)*$_{RBS}$ -3'	5'-**TA***(n)*$_{RBS}$ *AGATCTcatG*-3'	*Eco*RI/*Ase*I
NPT-F/R:	5'-**GATC***T(n)*$_{RBS}$ *atg(nnn)*$_{NPT}$ *g*-3'	5'-**TA***c(nnn)*$_{NPT}$ *cat(n)*$_{RBS}$ *A*-3'	*Bgl*II/*Ase*I
CPT-F/R:	5'-*ct(nnn)*$_{CPT}$ *taataataaG*-3'	5'-**GATC***Cttattatta(nnn)*$_{CPT}$ *agan*-3'	*Bpm*I/*Bam*HI
LIN-F/R:	5'-*ct(nnn)*$_{LIN}$ *g*-3'	5'-**TA***c(nnn)*$_{LIN}$ *agan*-3'	*Bpm*I/*Ase*I
RBS7-F:	5'-**AATT***CatgAGATCTaaataggaggaaaAT*-3'		*Eco*RI
RBS7-R:	5'-**TA***ATtttcctcctatttAGATCTcat*G-3'		*Ase*I
P1-F:	5'-gagG**AATT**CgTCTAGAtaccgtcgtggttaggccccccgggcccagaaaaatatttttt*caaaacccacttgacactttagc-3'*		*Eco*RI
P1-R:	5'-gacG**GATCC***tagcagcagatatcctctatagttattataaacatatata**gctaaagtgtcaagtgggttttg**-3'		*Bam*HI
P2-F:	5'-**AATT***CACTAGTcattctacagtttattcttgacattgcactgtccccctggtataataactatacatgcaaG*-3'		*Eco*RI
P2-R:	5'-**GATC***CttgcatgtatagttattataccaggggggacagtgcaatgtcaagaataaactgtagaatgACTAGTG*-3'		*Bam*HI
P3-F:	5'-**AATT***CACTAGTcattctacagtttattcttgacattgcactgtccccctggtataataactatacatgcaA*-3'		*Eco*RI
P3-R:	5'-**GATC***TtgcatgtatagttattataccaggggggacagtgcaatgtcaagaataaactgtagaatgACTAGTG*-3'		*Bgl*II
PZ1-F:	5'-gcaacG**AATT**CACTAG*Tgttagtcatatggacacttaaggc*-3'		*Eco*RI
PZ1-R:	5'-cgaacG**GATCC***ctagaaaagctgatattccaattgc*-3'		*Bam*HI
P_{fcsK}-F/R:	5'-catgG**AATT**C*aatcaattcaagtacacgttc*-3'	5'-catgG**GATCC***agaagtcgcacctaaatc*-3'	*Eco*RI/*Bam*HI
P_M -F/R:	5'-catgG**AATT**C*gtgctttgttacatataaattcaagc*-3'	5'-catgG**GATCC***gcacctcgtgtgttaaaataatg*-3'	*Eco*RI/*Bam*HI
P_{tre}-F/R:	5'-catgG**AATT**C*ttggatttgcttaaataattg*-3'	5'-catgG**GATCC***tgcatttgtaaaggttcc*-3'	*Eco*RI/*Bam*HI

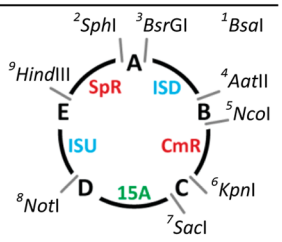

[a]CAPITAL, restriction recognition sequence; **bold**, sticky ends after digestion or oligo annealing; *italic*, homology sequence for annealing or PCR.

selection marker (in this case conferring chloramphenicol resistance; CmR) outside the integration sequence. Arrows in Figure 1A indicate reading directions for resistance cassettes and annotation directions of homology sequences and origin of replications.

For integration, the region between *amiF* and *treR* (Figure 1B) was selected because of its characteristics of a stable site without phenotypic consequences that allows for reliable gene expression.[13] AmiF is part of a membrane transport system for oligopeptides, and TreR is a transcriptional regulator of the trehalose operon. The intermediate *T1* and *T2* are residues of transposable elements. Upon integration, *T1* becomes truncated whereas all other genes remain intact. Homology loci span from base pair 1678030 to 1678505 for ISU and from base pair 1678908 to 1679400 for ISD according to the annotation in the *S. pneumoniae* D39 GenBank genome NC_008533.[14] These sequences are also perfect matches for D39 derivative strains such as R6. The positions of homology sequences differ slightly from the ones previously used in this locus[13] because of the requirement of an absence of BglBrick restriction sites. The distant position at 200° relative to the origin of replication (*oriC*) on the circular chromosome (20° removed from *ter* and 160° removed from *oriC*) is assumed to result in more stable expression when it comes to copy number effects due to DNA replication at exponential growth in contrast to ectopic integration close to the origin of replication.[15] Both upper and downer regions of homology were chosen at a length of approximately 500 bps. This length is a good compromise between integration efficiency[16] while maintaining a small vector backbone size.

The MCS was synthesized, and it includes recognition sequences for the BglBrick restriction sites *Eco*RI and *Bgl*II as prefix followed by *Bam*HI and *Xho*I as suffix. Furthermore, the BglBrick system was extended for direct assembly of translational units by adding *Ase*I and *Bpm*I to the system (described later). Additional restriction sites are present in the upstream part of the MCS that allow for the transfer of assembled constructs and that in general offer more cloning flexibility. Terminators were built in to ensure efficient termination of transcription and sufficient insulation of gene expression and to increase plasmid stability. Three synthetic terminators were obtained for this purpose from the iGEM parts registry[17] with BBa_B1002 and BBa_B0015 inside the MCS (notated as TER in Figure 1A) and a modified version of BBa_B1006 for the termination of BglBrick transcripts downstream of the MCS (right black circle in Figure 1A). For insulation of upstream transcription (left black circle in Figure 1A), two terminators of the D39 genome were chosen that originate from sequences following the genes for the ribosomal protein RpsI and the elongation factor Tuf.

Two origins of replication were added to the vector. The theta p15A origin of replication[18] was chosen for subcloning in *E. coli* with a narrow copy number distribution of 10−12 plasmids per cell; the template used was pSB3K3 from the parts registry. A standard kit-based plasmid prep of 4 mL of an overnight culture yields approximately 1500 ng of plasmid DNA which is sufficient for creation of backbone digests. The

dx.doi.org/10.1021/sb500229s | *ACS Synth. Biol.* 2015, 4, 228−239

Figure 2. Functional unit assembly in pPEP1. BglBrick assembly was chosen as standard with its four restriction sites *Eco*RI, *Bgl*II, *Bam*HI, and *Xho*I. Furthermore, the system was extended by the restriction sites *Ase*I and *Bpm*I to allow for an easy oligonucleotide-linker based exchange of RBSs, addition of peptide tags, or assembly of fusion proteins—the BglFusion format. Capital letters symbolize restriction recognition sites and bold restriction enzymes indicate positions where the backbone and inserts need to be cut and religated. Templates for the construction of oligonucleotide linkers are given in Table 1. Note that these are examples that suggest one way of how to assemble individual functional units and that alternatives are possible, offering maximal flexibility.

low to medium copy number has the advantage over high copy number plasmids that it reduces the chance of overexpression of potentially harmful gene products. Note that this origin does not allow for replication in *S. pneumoniae*. The second, broad host range, origin of replication is the low copy Ori$^+$ derived from the *Lactococcal* pWV01 rolling circle plasmid (template used: pORI28). However, the essential *repA* gene is omitted, and the origin of replication by itself is not functional.[19] This second origin of replication only becomes active when RepA is added *in trans* as is the case of *S. pneumoniae* D39*repA*[20] or *E. coli* EC1000.[21] With both origins of replication being functional, the absolute amount of plasmid DNA isolates increases from 380 ± 30 to 490 ± 40 ng/mL/OD when comparing MC1061 to the EC1000 host. This result indicates that there is no disruptive interference in the activity of the two origins of replication concerning plasmid stability.

The spectinomycin cassette of vector pAE03[22] was chosen for its characteristic as a reliable selection tool that works equally well in Gram-positive and Gram-negative backgrounds. The *Pst*I site was removed from the coding sequence through single base pair exchanges via assembly PCR (see Methods). Initial transformation assays gave rise to colonies in *E. coli* but not in *S. pneumoniae*. Since the spectinomycin resistance marker is placed directly downstream of the MCS and thus in proximity to strong terminators, we speculated that, in the absence of read-through transcription, the native promoter might not be strong enough to confer resistance after integration into *S. pneumoniae* at a single copy. Indeed, adding a synthetic constitutive promoter upstream of the *spec* marker solved the problem and integration into the pneumococcal genome worked successfully with transformation yields of approximately 5 × 10^5 CFU/OD per 30 ng of pPEP1 plasmid DNA.

Chloramphenicol acetyltransferase (CAT) of pNZ8048[23] was chosen as a marker outside the flanking homology regions. The *Mfe*I and *Ase*I sites were removed, as described. The main reason for adding the *cat* marker relies in easy screening for chloramphenicol sensitivity, which indicates successful double crossover (and loss of the *cat* marker) after initial selection on spectinomycin. Additionally, the presence of this marker makes it possible to select for single crossover integrants or even for plasmid propagation in *S. pneumoniae* carrying *repA in trans*.

Vector components ISU, SpR, ISD, CmR, and 15A were PCR amplified with *Bsa*I restriction sites creating non-palindromic sticky ends that were designed to be complementary to the following part in line (Table 1). Fragments were assembled using the protocols for Golden Gate Shuffling,[11] and products of this assembly reaction were PCR amplified to obtain higher DNA amounts. The PCR product of the subassembly ISU-SpR-ISD, representing the integration fraction, was successfully tested for transformation in *S. pneumoniae* and integration was verified by colony PCR with

dx.doi.org/10.1021/sb500229s | *ACS Synth. Biol.* 2015, 4, 228−239

Table 2. BglBricks in pPEP (BglFusion Format)

brick	description	plasmid	formatting action	reference
MCS	BglFusion cloning and transfer sites	pPEP1	synthesis	this study
Luc[a]	luciferase	pPEP2	PCR on p5.00; *Eco*RI site removed	Prudhomme et al., 2007[28]
GFP	sfGFP(*Bs*)	pPEP3	PCR on pKB01_sfgfp(*Bs*); *Bcl*I site removed	Overkamp et al., 2013[25]
mK2	mKate2	pPEP4	synthesis after codon optimization	Shcherbo et al., 2009[26]
P1	intermediate constitutive promoter	pPEP21	oligo extension PCR	this study
P2	strong constitutive promoter	pPEP22	oligo annealing	Jensen et al., 1998[29]
P3	very strong constitutive promoter	pPEP23	oligo annealing	Jensen et al., 1998[29]
PZ1	Zn^{2+}-inducible promoter	pPEP24	PCR on D39 genomic DNA	Eberhardt et al., 2009[22]
P_{fcsK}	fucose-inducible promoter	pPEP25	PCR on D39 genomic DNA	Chan et al., 2003
P_M	maltose-inducible promoter	pPEP26	PCR on D39 genomic DNA	Guiral et al., 2006
P_{tre}	trehalose-inducible promoter	pPEP27	PCR on D39 genomic DNA	Manzoor and Kuipers, unpublished

[a]Luc still contains two *Bpm*I sites.

the primer pair IF/IR (data not shown). The PCR amplified assembly of all five parts was subsequently digested with *Sph*I and *Bsr*GI and ligated to the MCS fragment that was cut out from its vector backbone coming from synthesis. In a second cloning step, the rolling circle origin of replication (Ori) was added by *Kpn*I and *Sac*I digestion and the final resulting vector (pPEP1) was transformed into *E. coli* strain MC1061 and sequence verified (GenBank accession number KF861544).

Functional Component Assembly. A fundamental principle of synthetic biology is the use of standardized parts to build up reliable gene regulatory functions. The standard chosen for the pPEP1 integration vector is BglBricks in form of translational and expression units. Figure 2A shows the general principle of this system with the example of assembling two genes into one translational unit. A more graphical representation of the BglBrick assembly principle can be found elsewhere.[9] In our system, we wanted to enable the transfer of BglBrick assembled expression units without simultaneously transferring any of the BglBrick restriction sites. This can be achieved by replacing the *Bgl*II site in promoter constructs with *Spe*I (or a compatible end creator like *Xba*I; Figure 2B). Expression units can now be cut with *Spe*I and *Bam*HI and ligated into the upstream part of the MCS of a different vector derived from pPEP1. We included terminator insulated transfer sites that create the required sticky ends with *Bsa*I + *Spe*I, *Xba*I + *Bcl*I or *Bcl*I + *Nhe*I (note that *Bsa*I creates *Bam*HI compatibility in the pPEP1 context). None of the BglBrick restriction sites re-establish in this process and the newly created vector can thus be used for further BglBrick cloning.

Arranging functional units in the form of ready-made translational units comes along with the limitation of predetermined RBSs and no flexibility for adding peptide tags or building up fusion proteins. These limitations can always be overcome by designing new primers amplifying the protein coding sequence (CDS) exclusively, with the scar of BglBrick assembly encoding for the linker residues glycine and serine. However, for our platform, we aim to incorporate the possibility of exchanging the mentioned components without the need of specific primers by introducing two more restriction enzymes to the system. *Ase*I was placed at the start of each CDS, with the last two bases of its recognition sequence (ATTAAT) overlapping with the first two bases of the start codon ATG. *Bpm*I, an offset cutter that cuts at a distance of 14 bps away from its recognition sequence, was positioned in between the suffix (*Bam*HI and *Xho*I) in such a way that it bridges the 3 stop codons that follow each CDS and in this process creates a sticky end out of the third base of the last amino acid codon and the first base of the first stop codon TAA. The two enzymes thus provide direct access to 5′ and 3′ ends of the CDS by simple restriction enzyme digestions. In both cases, two base pair overhangs are created, *Ase*I in 5′ and *Bpm*I in 3′, which lead to only one predetermination for amino acid linkers with valine and serine, respectively. In case that the two recognitions sequences cannot be eliminated in the CDS, one can sidestep to *Nde*I instead of *Ase*I and *Acu*I instead of *Bpm*I that give rise to similar patterns. This system extension of BglBrick cloning, we call it BglFusion, furthermore enables an easy parallelization of assembling multiple RBSs, peptide tags or linker-peptides in fusion proteins by ligating DNA constructs with linkers in form of annealed oligonucleotides (Figure 2C; Table 1).

To test our platform on its pledge of rapid cloning and robust and reliable gene expression inside the *S. pneumoniae* chromosome, we inserted the firefly luciferase gene *luc*,[24] sfGFP(*Bs*)[25] (from here on called GFP), and mKate2[26] into pPEP1 (Table 2). The BglFusion cloning site already carries an optimized RBS in the right position relative to *Ase*I for direct assembly of translational units. We nevertheless added a slightly different synthetic RBS, created with RBS7 oligonucleotides (Table 1), to demonstrate the feasibility of linker assisted cloning in our system. These synthetic RBSs were created with an optimized Shine−Dalgarno consensus sequence AGGAGG at a distance of 7 bps from the start codon and AT-rich sequences to reduce secondary structure formation.[27] Coding sequences were PCR amplified with *Ase*I restriction sites at the start codon and *Bam*HI restriction sites directly downstream of three stop codons TAA at the 3′ end of the genes. The pPEP1 vector backbone was cut with *Eco*RI and *Bam*HI, the coding sequences were cut with *Ase*I and *Bam*HI and the synthetic RBS was obtained by annealing oligonucleotides RBS7-F and RBS7-R that give rise to sticky ends compatibility for *Eco*RI and *Ase*I. Ligation mixtures of this cloning method resulted in efficient cloning yields in *E. coli*.

Construction and Characterization of a Standard Promoter Set. Bioluminescence as a result of luciferase activity from *luc* expression was chosen as the major reporter system for gene expression activity. The advantage of this technology above, for example, GFP measurements is the absence of background levels and distinguishable expression signals within 5 orders of magnitude. Furthermore, the half-life of the Luc protein is very short in *S. pneumoniae*;[28] thus, signals can directly be linked to promoter activity at a given time point and the system allows for easier evaluations of fast changing

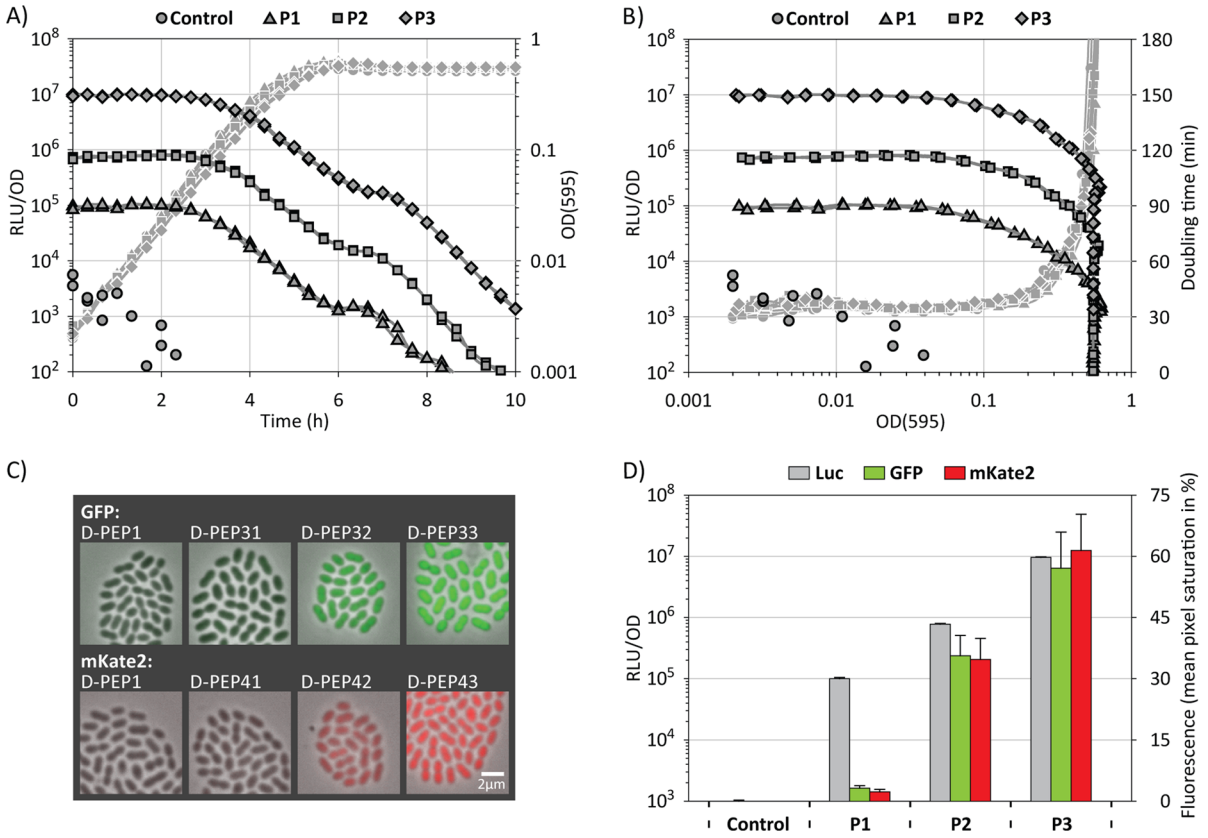

Figure 3. Characterization of a set of standard constitutive promoters for *S. pneumoniae*. (A) Plate reader assays measuring normalized luminescence (RLU/OD; au; closed symbols) and OD (symbols without outline) are plotted over time. (B) The same data set with RLU/OD (closed symbols) and doubling time (symbols without outline) plotted over OD. All assays are in duplicates including the control (circles, D-PEP1) and three constitutive promoters driving luciferase (triangles, P1/D-PEP21; squares, P2/D-PEP22; diamonds, P3/D-PEP23). (C) The same promoter set driving GFP and mKate2 in an overlay of phase contrast and fluorescence microscopy (scale bar = 2 μm). (D) Normalized luminescence (left axis) and normalized fluorescence (right axis) including population and cell-to-cell variations, respectively (standard deviations).

expression states. The biggest disadvantage compared to the widely used reporter GFP relies in the inability to collect single cell information with standard microscopy.

To construct gene regulatory networks with reliable gene expression strengths of the individual parts, well-characterized constitutive and controllable promoters are required. Six promoters of the Jensen et al. synthetic promoter library[29] for *E. coli* and *Lactococcus lactis* (in order of strength: CP4, CP1, CP26, CP46, CP7, CP6) were selected that represent a complete ladder of the spectrum of expression strength in their reported backgrounds. The main criteria of choice were similar expression behaviors in both *E. coli* and *L. lactis*, hence increasing the likelihood of conserved promoter sequence that work in multiple bacterial backgrounds. Surprisingly, four out of the six selected promoters gave no expression at all in *S. pneumoniae*. The results of Jensen et al. indicate that *L. lactis* is more constrained in promoter sequence recognition than *E. coli*. This trend might be carried forward in case of the pneumococcus that exhibits an even more reduced genome size. Of the two identified active promoters, CP1 gave rise to very weak signals close to the noise range (data not shown) and only CP26 resulted in high levels of bioluminescence from *luc* expression. The downstream border of this promoter was chosen tightly at position +8 relative to the transcriptional start. Interestingly, we observed different expression strengths depending on the sequence that directly followed this border, and this also influenced the choice of the restriction site connecting the promoter. Choosing the standard suffix *Bam*HI directly downstream of position +8 gives rise to the scar sequence GGATCT when ligated to a *Bgl*II digested reporter construct and we called this promoter P2. When eliminating the first G of *Bam*HI (+9 relative to transcriptional start) in contrast, then the last promoter base A from position +8 in combination with the remaining GATCT gives rise to *Bgl*II as promoter suffix instead. The re-established *Bgl*II recognition site AGATCT after ligation to a reporter construct results in a more than 10-fold higher gene expression activity of luciferase, and we sequentially called this promoter P3. To complete our library of constitutive promoters, we rationally designed and constructed another synthetic promoter: P1 consists of the prokaryotic consensus −35 (TTGACA) and −10 (TATAAT) sequences, the UP element 4171 from the Estrem et al. library[30] and the core sequence of P_{1-6Mt5} from the Liu et al. library[31] (Table 3).

Characterization of this standard set of constitutive promoters driving *luc* expression results in OD-normalized luciferase activities (RLU/OD) in the range from 10^5 to 10^7 arbitrary units. Each promoter is separated by 1 order of magnitude with promoter P1 being the weakest and P3 the strongest. Our constitutive promoter library displays a wide range of different expression strengths with similar promoter dynamics making them well suitable for synthetic biology approaches (Figure 3A−D). The promoter-less control of *luc* (D-PEP2) was also analyzed and gives rise to signals

dx.doi.org/10.1021/sb500229s | *ACS Synth. Biol.* 2015, 4, 228−239

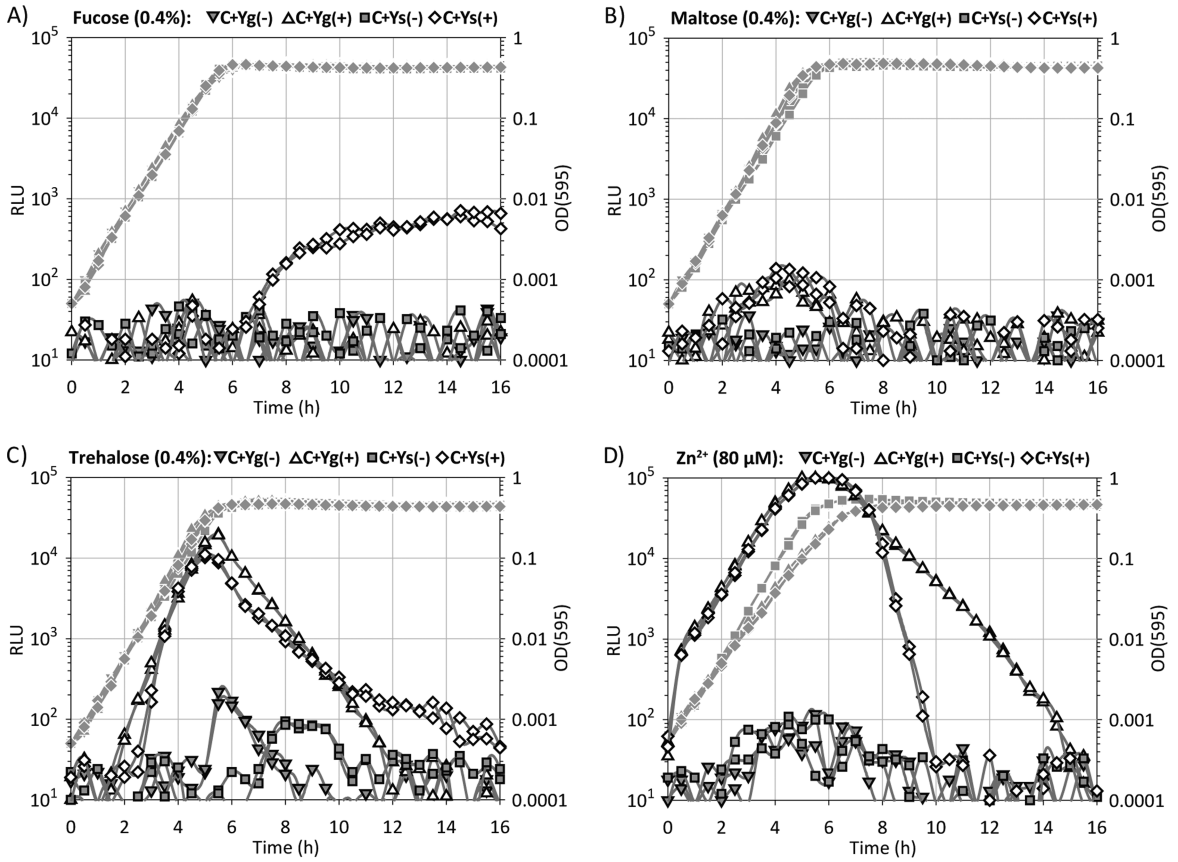

Figure 4. Comparison of four inducible promoters in *S. pneumoniae*. (A–D) Plate reader assay data sets in duplicates of the activity of the inducible promoters P_{fcsK} (A), P_M (B), P_{tre} (C), and PZ1 (D) driving luciferase in pPEP integration constructs in response to fucose, maltose, trehalose, and Zn^{2+}, respectively. Inducer concentrations were used that were shown previously to generate optimal expression.[13,34] Closed symbols represent luminescence (RLU; au) and symbols without outlines represent OD readings. Two different media were tested with C+Yg containing 0.4% glucose (triangles up and down) and C+Ys containing 0.2% sucrose (squares and diamonds) as main carbon source. Closed gray symbols (triangles down and squares) represent uninduced while closed white symbols (triangles up and diamonds) represent induced conditions (induction start is shortly before time point 0).

indistinguishable from cultures without luciferase or wells containing a medium blank; this demonstrates a very effective insulation of our expression locus. As shown in Figure 3D, the classical way of displaying gene expression levels as bar charts, although intuitive, only provides limited information on the behavior of promoters. Plotting bioluminescence as a function of time (Figure 3A) can also be misleading because time in contrast to cell density is only indirectly responsible for changes in promoter activity during batch cultivation. We therefore introduce a different kind of graph in which we plot the RLU/OD on a log scale on the *Y*-axis and the OD also in a log scale on the *X*-axis (Figure 3B). This illustration allows easy distinction of gene expression at different growth phases and thus in different environmental conditions. To demonstrate the functionality of our promoter set with different reporters, we also analyzed expression of GFP and the red fluorescent protein mKate2 (Figure 3C). This single cell analysis was carried out by fluorescence microscopy and computer aided evaluation of signal intensity with MicrobeTracker[32] (Figure 3D; Table 3). Our constitutive promoter library gives rise to a clear hierarchy in promoter strength for GFP and mKate2 (Figure 3D). The approximately 1 order of magnitude difference of the promoters in bioluminescence assays could be confirmed for fluorescent proteins in between P1 and P2 (factor 11 for GFP and factor 15 for mKate2). The difference between P2 and P3 with fluorescence reporters, however, is in the linear range resulting in approximately 2-fold higher mean signals (Figure 3D).

The above-mentioned results prompted us to conduct an analysis of the mRNA abundance to get a more detailed insight of transcription versus translation efficiencies in these constructs (Table 3). Transcript levels of the GFP expressing strains showed a 4-fold difference between P1 and P2 and a 2-fold difference between P2 and P3. We conclude that transcription is indeed higher in P3 compared to P2 (which is very similar in sequence) and that this increase in transcription is most probably responsible for the observed expression difference of fluorescence proteins. Possible explanations for the 10-fold increase of luciferase signals might include differences in translation efficiency, protein folding and maturation, fluorescent protein aggregation, or the fact that luciferase has a higher turnover rate.

Besides constitutive promoters, finely tunable inducible promoters are also indispensable for synthetic biology approaches. At this point there are only few examples for *S. pneumoniae* available such as the nisin-inducible P_{nis},[20] the ComS peptide-regulated system,[33] the carbon source promoters P_M[13] for maltose and P_{fcsK}[34] for fucose induction and the zinc-inducible P_{czcD}.[22] Here, we compared the two carbon source promoters to the unpublished P_{tre} that is activated by extracellular trehalose (Manzoor and Kuipers, unpublished

dx.doi.org/10.1021/sb500229s | *ACS Synth. Biol.* 2015, 4, 228–239

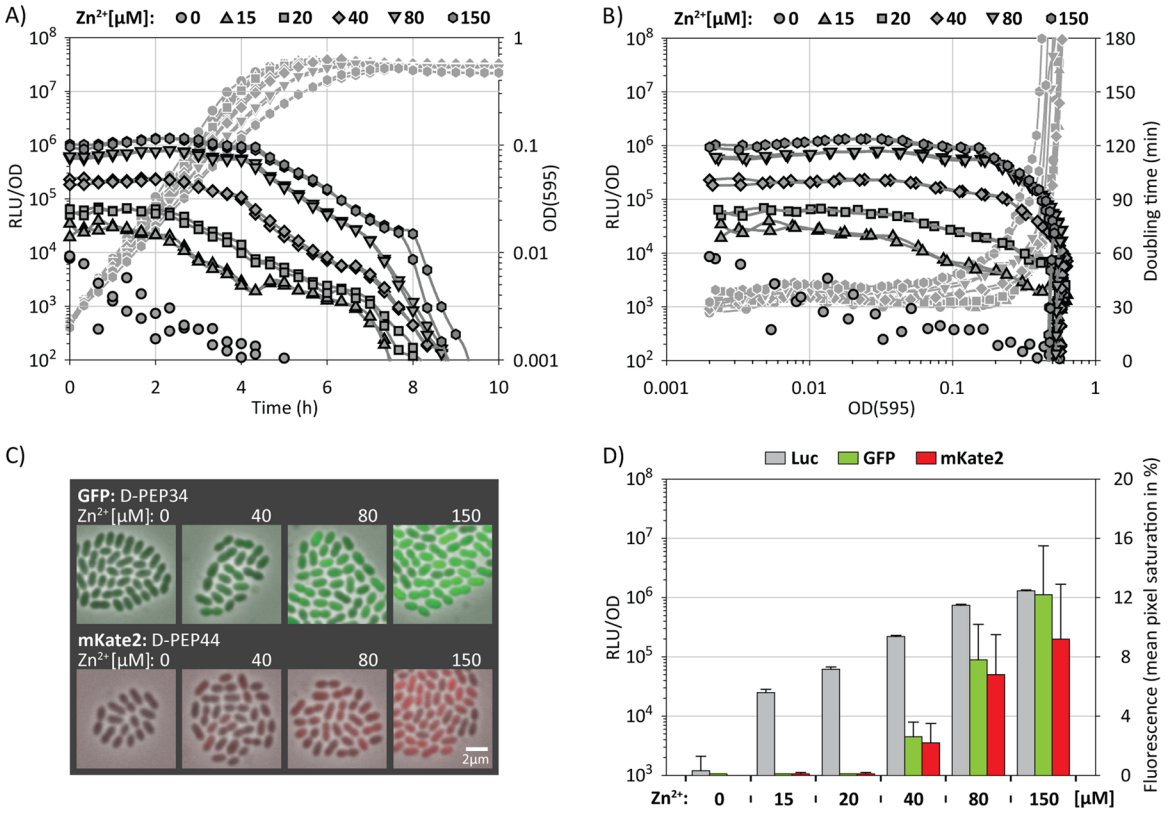

Figure 5. Characterization of the pneumococcal Zn^{2+}-inducible promoter. (A and B) Plate reader assays measuring normalized luminescence (RLU/OD; au; closed symbols) and OD (A) or doubling time (B) (symbols without outline) are plotted over time and OD, respectively. The data set shows duplicates of each of the six Zn^{2+} concentrations inducing luciferase expression from PZ1 in D-PEP24 (circles, 0; triangles up, 15; squares, 20; diamonds, 40; triangles down, 80; hexagons, 150 μM $ZnSO_4$). (C) Induction subset of the mentioned Zn^{2+} concentrations driving GFP and mKate2 in an overlay of phase contrast and fluorescence microscopy. (D) Summary of results, including population and cell-to-cell variations, respectively (standard deviations).

data) and additionally to a new version of P_{czcD} that was obtained by PCR amplification from D39 genomic DNA with more constraint borders than previously reported. Figure 4 shows growth curves of four strains with the mentioned inducible promoters driving luciferase in PEP integration constructs. Precultures were grown without inducer and time point 0 thus also represents the induction starting point. Plots are shown for concentrations of inducer that resulted in maximal reported expression levels.[13,34] Two different media were tested with C+Y containing 0.4% glucose (C+Yg) and containing 0.2% sucrose (C+Ys) as a main carbon source. Catabolite repression is presumably responsible for the observation that luciferase is not expressed from the fucose-inducible promoter in glucose medium but solely in stationary phase sucrose assays (Figure 4A). Furthermore, this phenomenon might also play a role in the differences in response timing and development in the case of the trehalose-inducible promoter (Figure 4C). Signals obtained with the maltose-inducible promoter in the pPEP background are generally very low (Figure 4B) and only the Zn^{2+}-inducible system shows consistently strong signals that develop in parallel to the OD (Figure 4D). A more in depth analysis of this promoter, renamed PZ1, showed a clear concentration dependent behavior in the range from 0 to 150 μM Zn^{2+} using $ZnSO_4$ as inducing chemical (Figure 5). However, $ZnSO_4$ concentrations of 80 μM and higher need to be treated with care since there is a negative effect on cell growth (Figure 5A). Single cell analysis with both GFP and mKate2 showed that this promoter gives rise to much more noise in gene expression compared to our constitutive promoters, with an up to factor two increase of the standard deviation at comparable mean values. Expression from these two fluorescence reporters displays a high degree of consistency in terms of trend when comparing expression strength within one promoter set. This was also confirmed by an analysis of the mRNA abundance in the GFP expressing strain (Table 3). Note that a detectable resolution of fluorescence signals for Zn^{2+} concentrations below 40 μM was not achieved. This might be explained by high background and noise levels dominating over low signals. In the case of luminescence, the signal-to-noise ratio is approximately 2 orders of magnitude higher and therefore enables the detection of significant results for the low Zn^{2+} concentration range. Cross-comparing between our sets from constitutive to the inducible promoter do not always show the expected expression values. This observation can be explained by the fact that the assembling of these promoters to a specific reporter always gives rise to individual connecting sequences. These sequences can act as proximal promoters fractions and thus influence transcription efficiency, or as 5′UTRs and thus influence mRNA stability and translation efficiency, a phenomenon well described recently.[35] In particular, while PZ1 induced with 80 μM of Zn^{2+} gives rise to significantly more transcript than for instance P3, the total amount of reporter protein produced is much higher from P3 indicating better translation signals for the latter (Table 3).

dx.doi.org/10.1021/sb500229s | ACS Synth. Biol. 2015, 4, 228−239

Table 3. Promoter Characterization Data

name	description	strain	RLU/OD[a]	strain	mRNA[b]	GFP[c]	strain	mK2[c]
	control	D-PEP1	$2.6\times10^{2} \pm 7.8\times10^{2}$	D-PEP1	0.0 ± 0.0	7.9 ± 0.2	D-PEP1	6.3 ± 0.0
P1	intermediate	D-PEP21	$1.0\times10^{5} \pm 5.2\times10^{3}$	D-PEP31	12.1 ± 0.9	3.2 ± 0.6	D-PEP41	2.3 ± 0.6
P2	strong	D-PEP22	$7.8\times10^{5} \pm 2.3\times10^{4}$	D-PEP32	45.0 ± 6.0	35.6 ± 5.0	D-PEP42	34.7 ± 5.2
P3	very strong	D-PEP23	$9.6\times10^{6} \pm 1.3\times10^{5}$	D-PEP33	86.2 ± 5.1	57.1 ± 8.8	D-PEP43	61.4 ± 8.9
PZ1	Zn^{2+}: 0 μM	D-PEP24	$1.2\times10^{3} \pm 9.0\times10^{2}$	D-PEP34	1.0 ± 0.1	0.1 ± 0.0	D-PEP44	0.0 ± 0.0
PZ1	Zn^{2+}: 15 μM	D-PEP24	$2.5\times10^{4} \pm 3.4\times10^{3}$	D-PEP34	n/a	0.1 ± 0.0	D-PEP44	0.1 ± 0.1
PZ1	Zn^{2+}: 20 μM	D-PEP24	$6.2\times10^{4} \pm 5.9\times10^{3}$	D-PEP34	6.4 ± 1.0	0.1 ± 0.0	D-PEP44	0.1 ± 0.1
PZ1	Zn^{2+}: 40 μM	D-PEP24	$2.2\times10^{5} \pm 1.1\times10^{4}$	D-PEP34	36.1 ± 2.7	2.6 ± 1.0	D-PEP44	2.2 ± 1.3
PZ1	Zn^{2+}: 80 μM	D-PEP24	$7.4\times10^{5} \pm 3.2\times10^{4}$	D-PEP34	130.1 ± 9.3	7.8 ± 2.4	D-PEP44	6.8 ± 2.7
PZ1	Zn^{2+}: 150 μM	D-PEP24	$1.3\times10^{6} \pm 4.9\times10^{4}$	D-PEP34	n/a	12.2 ± 3.3	D-PEP44	9.2 ± 3.7

P1[d]	GAAAAAATATTTTTCAAAACCCAC **TTGACA**CTTTAGCTATATATGTT**TATAAT**AACTAT **G**AGGATATCTGCTGCTAGGATCTAAAT**AGGAGG**AAAATTA**ATG**
P2	CACTAGTCATTCTACAGTTTATTC **TTGACA**TTGCACTGTCCCCCTGG**TATAAT**AACTAT **A**CATGCAAGGATCTAAAT**AGGAGG**AAAATTA**ATG**
P3	CACTAGTCATTCTACAGTTTATTC **TTGACA**TTGCACTGTCCCCCTGG**TATAAT**AACTAT **A**CATGCAA-GATCTAAAT**AGGAGG**AAAATTA**ATG**
PZ1	TGAATAAAGCTGACGTTTTGCTTC TATCCTTTCTTTGAGTTTTAGTG**GATAAT**GATAAT **G**AACAAGGTGTTCA(N)$_{200}$TAAAT**AGGAGG**AAAATTA**ATG**

[a]OD normalized luminescence ± population standard deviation. [b]Relative mRNA abundance ± standard deviation of qPCR replicates. [c]Fluorescence: mean pixel saturation of cell area (%) ± cell to cell variation. [d]Promoter sequences: −35, −10, +1, RBS, and ATG in bold.

In total, we have generated a set of standardized characterized constitutive promoters and an inducible promoter with a high dynamic range (Figures 3 and 5), which can serve as excellent starting point for synthetic biology approaches in *S. pneumoniae*.

Concluding Remarks. In this study, we initially constructed a vector backbone including all desired features *in silico* and ordered it from DNA synthesis. However, for reasons unknown, the delivered plasmid worked fine in *E. coli* but did not transform efficiently to *S. pneumoniae*. One possible explanation might be found in the mentioned insufficiency of resistance gene expression. The experience gained in this project shows that *de novo* synthesis of an entire plasmid (or a complete bacterial genome for that matter[36]) is a risky business since it does not guarantee a working system. Current methods of multipart assembly such as USER assembly,[37] Gibson assembly[38] or the here applied Golden Gate Shuffling[11] offer an alternative strategy to build up new vectors and facilitate easy reshuffling with alternative components and rapid troubleshooting.

The here developed gene expression platform for *S. pneumoniae* by multipart assembly has several key features:

- standardization of genetic units with the BglFusion format,
- fast and easy assembly of coding sequences and promoters,
- free shuffling of RBSs, peptide tags and linkers in fusion proteins,
- robust plasmid propagation at stable copy numbers of 10−12 in *E. coli*,
- efficient and reliably integration into the *S. pneumoniae* genome,
- plasmid propagation in prokaryotic backgrounds ectopically expressing RepA.

In addition to the generation of pPEP1 and derivatives, we present a method for visualizing the dynamic environment that cells experience during a typical growth experiment by plotting gene expression profiles as RLU/OD against OD in a double logarithmic graph. Constitutive gene expression from our promoters in general did shutdown significantly before one could observe a decrease in cell doubling time. Growth limiting environments thus seem to impact gene expression earlier than cell growth, displaying a surplus of factors that allow for continued growth before limitations become visible and transition to stationary phase occurs.

It was surprising to find that several promoters leading to high gene expression in *E. coli* and *L. lactis* gave no signals in *S. pneumoniae*. This phenomenon is another striking demonstration of the individuality of gene expression in different organisms, while relying on similar fundamental core components. It also displays the limit of synthetic biology applicability with the idea of units that can be freely transferred from one organism to another while maintaining the same functionality. In reality, there appears to be the need of redesigning the standards for each new genetic background, whereupon the strategies and techniques of doing so can be transferred. This is exactly what we wanted to achieve with this study. We have successfully constructed a new genetic integration platform for *S. pneumoniae* that allows for rapid and robust BglBrick assembly and have made a first start at developing and characterizing a set of standard promoters and reporters for synthetic biology purposes in this organism. The here described genetic platform, methods, and promoters will enable the design and construction of more complex gene regulatory circuitries, such as feedback systems or toggle switches, which might eventually contribute to our understanding of the gene regulatory networks underlying virulence development in this important human pathogen.

METHODS

Strains, Transformations, and Growth Conditions. All strains are derived from MC1061 in *E. coli* and D39 in *S. pneumoniae*. All constructs were subcloned in *E. coli*; competent cells were obtained by $CaCl_2$ treatment according to Sambrook and Russell.[39] *E. coli* was transformed via heat-shock at 42 °C for 2 min and *S. pneumoniae* with 1 ng/mL CSP (competence stimulating peptide) at OD 0.1 according to standard protocols.[40] Cells were plated in the presence of 100 μg/mL spectinomycin on LB-agar and Columbia agar (supplemented with 3% (v/v) sheep blood) respectively and incubated at 37 °C for selection of positive transformants. *E. coli* colonies were

dx.doi.org/10.1021/sb500229s | *ACS Synth. Biol.* 2015, 4, 228−239

picked and grown overnight in LB medium containing 100 μg/mL spectinomycin. *S. pneumoniae* colonies were restreaked by plating inside Columbia agar; colonies were subsequently picked and grown in C+Y[41] (pH 6.8) until OD 0.4 to obtain −80 °C glycerol stocks.

Vector and Functional Unit Assembly; Restriction Site Removal. Individual vector components were PCR-amplified using high fidelity Phusion polymerase (Thermo Fisher Scientific, Waltham, MA, U.S.A.) as described in the main text and assembled according to the Golden Gate Shuffling protocol.[11] Unwanted restriction sites were eliminated through single base pair silent mutations by PCR assembly of upstream and downstream PCR products that overlap approximately 25 bps around the altered sites. The MCS was synthesized by GenScript (Piscataway, NJ, U.S.A.) as part of a full plasmid synthesis (see Concluding Remarks). The RBS7, P2, and P3 were obtained with oligonucleotides that were designed for both homologous strands with the addition of the required single stranded sticky ends. Annealing reactions were carried out in FD-buffer (Thermo Fisher Scientific) containing 20 μM of each oligonucleotide. Reaction tubes were heated to 98 °C and slowly cooled to room temperature. P1 was created with oligonucleotides that overlap 23 bps by polymerase driven extension, and thus the creation of double stranded DNA. After digestion with FD enzymes (Thermo Fisher Scientific), individual components were column- or gel-purified, ligated, and transformed into *E. coli*.

Microtiter Plate Reader Assays. Precultures were inoculated from −80 °C stocks to OD 0.005 and grown until OD 0.1 in 2 mL C+Y medium (pH 6.8) at 37 °C inside 5 mL red cap tubes that allow for direct in tube OD measurement. Note that *S. pneumoniae* induces autolysis when kept in stationary phase at 37 °C for longer periods and dilution of late logarithmic cultures will generate variable lag phases and therefore should be omitted when possible. Costar 96-well plates (white, clear bottom) with a total assay volume of 300 μL C+Y per well supplemented with 0.5 μg/mL D-luciferine were inoculated to the designated starting OD value. Microtiter plate reader experiments were performed using a TECAN infinite pro 200 plate reader (Tecan Group, Männedorf, Switzerland) by measuring every 10 min with the following protocol: 5 s shaking; OD(595) measurement with 25 flashes; luminescence measurement with an integration time of 1 s. Doubling times were obtained by calculating an average of OD developments of 1, 2, and 3 measurement points preceding and following the current value with a weighting of 1, $^1/_2$, and $^1/_4$, respectively. Specific RLU/OD values for the bar graph were obtained by the average and the standard deviation of measurement values in the OD range from 0.01 to 0.03 coming from both duplicates.

Microscopy and MicrobeTracker Analysis. Precultures for microscopy were obtained as described above for plate reader assays. Strains containing PZ1 were induced for 75 min by diluting the initial preculture factor 8 and regrowing them to OD 0.1 in the presence of Zn^{2+}. Cell metabolism was stopped by placing the tubes on ice, and medium was exchanged by spinning down 1 mL of growth culture and resuspension in 200 μL PBS. After thorough vortexing, 1 μL of the cell preparation was spotted on a PBS-polyacrylamide (10%) slide inside a Gene Frame (Thermo Fisher Scientific) and sealed with the cover glass to guaranty stable conditions during microscopy. A Nikon Ti-E microscope equipped with a CoolsnapHQ2 camera and an Intensilight light source was used. Images with GFP fluorescing cells were taken with the following protocol and filter set: 200 ms exposure time for phase contrast; 1 and 0.5 s exposures (two measurements in case of pixel oversaturation) for fluorescence at 450−490 nm excitation via a dichroic mirror of 495 nm and an emission filter at 500−550 nm. Images of mKate2 fluorescing cells were obtained by the same protocol with the difference of 500 ms exposure time for phase contrast and a filter set of 560−600 nm for excitation, dichroic mirror of 605 nm, and emission of >615 nm (long-pass filter). More than 200 cells in average were computationally analyzed per condition with the MATLAB based software MicrobeTracker.[32] In brief, cells are identified based on phase contrast pictures, and the selected areas are analyzed in the respective fluorescence picture. Fluorescence signals coming from the 0.5 s exposure time were cell area normalized and averages and standard deviations were calculated. Figure 3C shows cells from 0.5 s exposure time while the 1 s exposure time was chosen for Figure 5C due to weaker signals.

mRNA Extraction, Reverse Transcription, and qPCR. Cultures for RNA isolation were inoculated and grown as described above and volumes of 8 mL were harvested at OD 0.1. RNA was isolated using the High Pure RNA Isolation Kit (Roche Applied Science, Penzberg, Germany) according to protocol with the addition of a 45 min DNase I treatment at 37 °C in the presence of the RNase inhibitor RiboLock (Thermo Fisher Scientific). Reverse transcription was performed using random nonamer primers and SuperScript III Reverse Transcriptase (Invitrogen, Carlsbad, CA, U.S.A.). Quantitative PCR (qPCR) experiments were carried out with iQ SYBR Green Supermix and a iQ5Multicolor Real-Time PCR machine (Bio-Rad Laboratories, Hercules, CA, U.S.A.). Primer sequences were obtained with the Primer3Plus software;[42] they exhibited identical calculated annealing temperatures and resulted in product sizes of approximately 100 bps. Samples were analyzed in quadruplicate with three primer sets including the housekeeping gene *gyrA*, the constitutively expressed spectinomycin resistance gene *SpR* from the pPEP platform and the gene of interest *gfp*. For each sample, the result for *gfp* was normalized to the average of the results for the internal controls *gyrA* and *SpR*. Finally, the quantities of all samples were normalized to sample D-PEP34 at 0 μM Zn^{2+}.

AUTHOR INFORMATION

Corresponding Author

*Tel.: +31 050 3632408. Fax: +31 050 3632348. Email: j.w.veening@rug.nl.

Notes

The authors declare no competing financial interest.

ACKNOWLEDGMENTS

Work in the Veening lab is supported by a VIDI fellowship (864.12.001) from The Netherlands Organisation for Scientific Research, Earth and Life Sciences (NWO-ALW) and the ERC starting grant 337399-PneumoCell.

REFERENCES

(1) Regev-Yochay, G., Raz, M., Dagan, R., Porat, N., Shainberg, B., Pinco, E., Keller, N., and Rubinstein, E. (2004) Nasopharyngeal carriage of *Streptococcus pneumoniae* by adults and children in community and family settings. *Clin. Infect. Dis. 38*, 632−639.

(2) Levine, H., Balicer, R. D., Zarka, S., Sela, T., Rozhavski, V., Cohen, D., Kayouf, R., Ambar, R., Porat, N., and Dagan, R. (2012) Dynamics of Pneumococcal acquisition and carriage in young adults

during training in confined settings in Israel. *PLoS One 7*, e46491 DOI: 10.1371/journal.pone.0046491.
(3) Weiser, J. N. (2010) The pneumococcus: Why a commensal misbehaves. *J. Mol. Med. Berl. Ger. 88*, 97−102.
(4) O'Brien, K. L., Wolfson, L. J., Watt, J. P., Henkle, E., Deloria-Knoll, M., McCall, N., Lee, E., Mulholland, K., Levine, O. S., Cherian, T., and Hib and Pneumococcal Global Burden of Disease Study Team (2009) Burden of disease caused by *Streptococcus pneumoniae* in children younger than 5 years: Global estimates. *Lancet 374*, 893−902.
(5) Bashor, C. J., Horwitz, A. A., Peisajovich, S. G., and Lim, W. A. (2010) Rewiring cells: Synthetic biology as a tool to interrogate the organizational principles of living systems. *Annu. Rev. Biophys. 39*, 515−537.
(6) Erwin, A. L., Brewah, Y. A., Couchenour, D. A., Barren, P. R., Burke, S. J., Choi, G. H., Lathigra, R., Hanson, M. S., and Weiser, J. N. (2000) Role of lipopolysaccharide phase variation in susceptibility of *Haemophilus influenzae* to bactericidal immunoglobulin M antibodies in rabbit sera. *Infect. Immun. 68*, 2804−2807.
(7) Cağatay, T., Turcotte, M., Elowitz, M. B., Garcia-Ojalvo, J., and Süel, G. M. (2009) Architecture-dependent noise discriminates functionally analogous differentiation circuits. *Cell 139*, 512−522.
(8) Khalil, A. S., and Collins, J. J. (2010) Synthetic biology: Applications come of age. *Nat. Rev. Genet. 11*, 367−379.
(9) Anderson, J. C., Dueber, J. E., Leguia, M., Wu, G. C., Goler, J. A., Arkin, A. P., and Keasling, J. D. (2010) BglBricks: A flexible standard for biological part assembly. *J. Biol. Eng. 4*, 1.
(10) Knight T. F. *Idempotent Vector Design for Standard Assembly of Biobricks*. http://hdl.handle.net/1721.1/21168 (accessed 01-05-2013).
(11) Engler, C., Gruetzner, R., Kandzia, R., and Marillonnet, S. (2009) Golden gate shuffling: A one-pot DNA shuffling method based on type IIs restriction enzymes. *PloS One 4*, e5553.
(12) Avery, O. T., Macleod, C. M., and McCarty, M. (1944) Studies on the chemical nature of the substance inducing transformation of pneumococcal types: Induction of transformation by a desoxyribonucleic acid fraction isolated from pneumococcus type III. *J. Exp. Med. 79*, 137−158.
(13) Guiral, S., Hénard, V., Laaberki, M.-H., Granadel, C., Prudhomme, M., Martin, B., and Claverys, J.-P. (2006) Construction and evaluation of a chromosomal expression platform (CEP) for ectopic, maltose-driven gene expression in *Streptococcus pneumoniae*. *Microbiology 152*, 343−349.
(14) Lanie, J. A., Ng, W.-L., Kazmierczak, K. M., Andrzejewski, T. M., Davidsen, T. M., Wayne, K. J., Tettelin, H., Glass, J. I., and Winkler, M. E. (2007) Genome sequence of Avery's virulent serotype 2 strain D39 of *Streptococcus pneumoniae* and comparison with that of unencapsulated laboratory strain R6. *J. Bacteriol. 189*, 38−51.
(15) Slager, J., Kjos, M., Attaiech, L., and Veening, J. V. (2014) Antibiotic-induced replication stress triggers bacterial competence by increasing gene dosage near the origin. *Cell 157*, 395−406.
(16) Lee, M. S., Seok, C., and Morrison, D. A. (1998) Insertion-duplication mutagenesis in *Streptococcus pneumoniae*: Targeting fragment length is a critical parameter in use as a random insertion tool. *Appl. Environ. Microbiol. 64*, 4796−4802.
(17) Registry for Standard Biological Parts. http://parts.igem.org/Main_Page?title=Main_Page (accessed 01-05-2013).
(18) Selzer, G., Som, T., Itoh, T., and Tomizawa, J. (1983) The origin of replication of plasmid p15A and comparative studies on the nucleotide sequences around the origin of related plasmids. *Cell 32*, 119−129.
(19) Leenhouts, K. J., Kok, J., and Venema, G. (1991) Lactococcal plasmid pWV01 as an integration vector for lactococci. *Appl. Environ. Microbiol. 57*, 2562−2567.
(20) Kloosterman, T. G., Bijlsma, J. J. E., Kok, J., and Kuipers, O. P. (2006) To have neighbor's fare: Extending the molecular toolbox for *Streptococcus pneumoniae*. *Microbiology 152*, 351−359.
(21) Leenhouts, K., Buist, G., Bolhuis, A., ten Berge, A., Kiel, J., Mierau, I., Dabrowska, M., Venema, G., and Kok, J. (1996) A general system for generating unlabelled gene replacements in bacterial chromosomes. *Mol. Gen. Genet. 253*, 217−224.
(22) Eberhardt, A., Wu, L. J., Errington, J., Vollmer, W., and Veening, J.-W. (2009) Cellular localization of choline-utilization proteins in *Streptococcus pneumoniae* using novel fluorescent reporter systems. *Mol. Microbiol. 74*, 395−408.
(23) Ruyter, P. G. de, Kuipers, O. P., and de Vos, W. M. (1996) Controlled gene expression systems for *Lactococcus lactis* with the food-grade inducer nisin. *Appl. Environ. Microbiol. 62*, 3662−3667.
(24) Stieger, M., Wohlgensinger, B., Kamber, M., Lutz, Rolf, and Keck, W. (1999) Integrational plasmids for the tetracycline-regulated expression of genes in *Streptococcus pneumoniae*. *Gene 226*, 243−251.
(25) Overkamp, W., Beilharz, K., Detert Oude Weme, R., Solopova, A., Karsens, H., Kovács, A. T., Kok, J., Kuipers, O. P., and Veening, J.-W. (2013) Benchmarking various green fluorescent protein variants in *Bacillus subtilis*, *Streptococcus pneumoniae*, and *Lactococcus lactis* for live cell imaging. *Appl. Environ. Microbiol. 79*, 6481−6490.
(26) Shcherbo, D., Murphy, C. S., Ermakova, G. V., Solovieva, E. A., Chepurnykh, T. V., Shcheglov, A. S., Verkhusha, V. V., Pletnev, V. Z., Hazelwood, K. L., Roche, P. M., Lukyanov, S., Zaraisky, A. G., Davidson, M. W., and Chudakov, D. M. (2009) Far-red fluorescent tags for protein imaging in living tissues. *Biochem. J. 418*, 567.
(27) Salis, H. M., Mirsky, E. A., and Voigt, C. A. (2009) Automated design of synthetic ribosome binding sites to control protein expression. *Nat. Biotechnol. 27*, 946−950.
(28) Prudhomme, M. and Claverys, J. P. (2007) There will be a light: the use of *luc* transcriptional fusions in living pneumococcal cells. *In The Molecular Biology of Streptococci.* Hakenbeck, R., and Chhatwal, G. S., Eds.; Horizon Scientific Press, Norfolk, U.K; pp 591−524.
(29) Jensen, P. R., and Hammer, K. (1998) The sequence of spacers between the consensus sequences modulates the strength of prokaryotic promoters. *Appl. Environ. Microbiol. 64*, 82−87.
(30) Estrem, S. T., Gaal, T., Ross, W., and Gourse, R. L. (1998) Identification of an UP element consensus sequence for bacterial promoters. *Proc. Natl. Acad. Sci. U.S.A. 95*, 9761−9766.
(31) Liu, M., Tolstorukov, M., Zhurkin, V., Garges, S., and Adhya, S. (2004) A mutant spacer sequence between −35 and −10 elements makes the Plac promoter hyperactive and cAMP receptor protein-independent. *Proc. Natl. Acad. Sci. U.S.A. 101*, 6911−6916.
(32) Sliusarenko, O., Heinritz, J., Emonet, T., and Jacobs-Wagner, C. (2011) High-throughput, subpixel precision analysis of bacterial morphogenesis and intracellular spatio-temporal dynamics. *Mol. Microbiol. 80*, 612−627.
(33) Berg, K. H., Biørnstad, T. J., Straume, D., and Håvarstein, L. S. (2011) Peptide-regulated gene depletion system developed for use in *Streptococcus pneumoniae*. *J. Bacteriol. 193*, 5207−5215.
(34) Chan, P. F., O'Dwyer, K. M., Palmer, L. M., Ambrad, J. D., Ingraham, K. A., So, C., Lonetto, M. A., Biswas, S., Rosenberg, M., Holmes, D. J., and Zalacain, M. (2003) Characterization of a novel fucose-regulated promoter (PfcsK) suitable for gene essentiality and antibacterial mode-of-action studies in *Streptococcus pneumoniae*. *J. Bacteriol. 185*, 2051−2058.
(35) Mutalik, V. K., Guimaraes, J. C., Cambray, G., Mai, Q.-A., Christoffersen, M. J., Martin, L., Yu, A., Lam, C., Rodriguez, C., Bennett, G., Keasling, J. D., Endy, D., and Arkin, A. P. (2013) Quantitative estimation of activity and quality for collections of functional genetic elements. *Nat. Methods 10*, 347−353.
(36) Gibson, D. G., Glass, J. I., Lartigue, C., Noskov, V. N., Chuang, R.-Y., Algire, M. A., Benders, G. A., Montague, M. G., Ma, L., Moodie, M. M., Merryman, C., Vashee, S., Krishnakumar, R., Assad-Garcia, N., Andrews-Pfannkoch, C., Denisova, E. A., Young, L., Qi, Z.-Q., Segall-Shapiro, T. H., Calvey, C. H., Parmar, P. P., Hutchison, C. A., 3rd, Smith, H. O., and Venter, J. C. (2010) Creation of a bacterial cell controlled by a chemically synthesized genome. *Science 329*, 52−56.
(37) Bitinaite, J., Rubino, M., Varma, K. H., Schildkraut, I., Vaisvila, R., and Vaiskunaite, R. (2007) USER friendly DNA engineering and cloning method by uracil excision. *Nucleic Acids Res. 35*, 1992−2002.
(38) Gibson, D. G., Young, L., Chuang, R.-Y., Venter, J. C., Hutchison, C. A., 3rd, and Smith, H. O. (2009) Enzymatic assembly of DNA molecules up to several hundred kilobases. *Nat. Methods 6*, 343−345.

(39) Sambrook, J., and Russell, D. W. (2001) *Molecular Cloning: A Laboratory Manual*. Cold Spring Harbor Laboratory Press, Cold Spring Harbor, NY.
(40) Martin, B., Prudhomme, M., Alloing, G., Granadel, C., and Claverys, J. P. (2000) Cross-regulation of competence pheromone production and export in the early control of transformation in *Streptococcus pneumoniae*. *Mol. Microbiol. 38*, 867−878.
(41) Bergé, M., Moscoso, M., Prudhomme, M., Martin, B., and Claverys, J.-P. (2002) Uptake of transforming DNA in Gram-positive bacteria: A view from *Streptococcus pneumoniae*. *Mol. Microbiol. 45*, 411−421.
(42) Untergasser, A., Cutcutache, I., Koressaar, T., Ye, J., Faircloth, B. C., Remm, M., and Rozen, S. G. (2012) Primer3—New capabilities and interfaces. *Nucleic Acids Res. 40*, e115.